Identification of Tyrosine Residues Involved in Ligand Recognition by the Phosphatidylinositol 3-Kinase Src Homology 3 Domain: Circular Dichroism and UV Resonance Raman Studies†

Nobuyuki Okishio,‡ Toshiyuki Tanaka,§ Masako Nagai,|| Ryuji Fukuda,‡ Shigenori Nagatomo,⊥ and Teizo Kitagawa*,⊥

Department of Biochemistry, School of Medicine, Kanazawa University Faculty of Medicine, Kanazawa, Ishikawa 920-8640, Japan, Institute of Applied Biochemistry and Center for Tsukuba Advanced Research Alliance, University of Tsukuba, Tsukuba, Ibaraki 305-8572, Japan, School of Health Sciences, Kanazawa University Faculty of Medicine, Kanazawa, Ishikawa 920-0942, Japan, and Institute for Molecular Science, Okazaki National Research Institutes, Myodaiji, Okazaki 444-8585, Japan

Received June 26, 2001; Revised Manuscript Received October 8, 2001

ABSTRACT: Src homology 3 (SH3) domains are small noncatalytic protein modules capable of mediating protein−protein interactions. We previously demonstrated that the association of a ligand peptide RLP1 (RKLPPRPSK) causes environmental and structural changes of Trp55 and some of seven Tyr residues in the phosphatidylinositol 3-kinase (PI3K) SH3 domain by circular dichroism (CD) and 235-nm excited UV resonance Raman (UVRR) spectroscopies [Okishio, N., et al. (2000) *Biopolymers 57*, 208−217]. In this work, the affected Tyr residues were identified as Tyr12, Tyr14, and Tyr73 by the CD analysis of a series of mutants, in which every single Tyr residue was replaced by a Phe residue. Among these three residues, Tyr14 was found to be a main contributor to the UVRR spectral change upon the RLP1 binding. Interestingly, CD and UVRR analyses revealed that RLP1 associates with the Y14F and Y14H mutants in different ways. These results suggest that Tyr14 plays a crucial role in the ligand recognition, and the amino acid substitution at Tyr14 affects the mode of PI3K SH3−ligand interaction. Our findings give an insight into how SH3 domains can produce diversity and specificity to transduce signaling within cells.

The class IA phosphatidylinositol 3-kinase (PI3K)[1] is a heterodimeric enzyme composed of a noncatalytic 85 kDa (p85) subunit and a catalytic 110 kDa (p110) subunit that contains PI3K and serine kinase activities. The noncatalytic subunit has several functional domains including a Src homology 3 (SH3) domain, a breakpoint cluster region homology domain, two proline-rich regions, and two Src homology 2 domains. This structural feature denotes that p85 may have multiple interactive and regulatory functions (*1*, *2*). For example, several proteins such as dynamin (*3*), CDC42GAP (*4*), Shc (*5*), and FAK (*6*) have been identified to interact with the p85 SH3 domain (the PI3K SH3 domain). This indicates that the PI3K SH3 domain plays important roles in signal transduction pathways.

UV resonance Raman (UVRR) spectroscopy is a powerful technique to selectively examine environmental and structural changes of aromatic residues in proteins (*7*−*10*). This method so far has been used to elucidate roles of particular aromatic residues in hemoglobin cooperativity (*11*−*14*) and to detect phosphorylation-induced microstructural changes of a Tyr residue in two kinds of Src-derived peptides (*15*).

In the previous study (*16*), we applied 235-nm excited UVRR spectroscopy in combination with circular dichroism (CD) to examine environmental and structural changes of Trp and Tyr residues in the PI3K SH3 domain induced by the association of a ligand peptide RLP1 (RKLPPRPSK) (*17*), and we revealed that Trp55 and some of seven Tyr residues are involved in the RLP1 interaction. In this work, we specified the responsible Tyr residues with the use of a series of Tyr → Phe (Y → F) mutants and the Y14H (Tyr14 → His) mutant. The mechanisms by which SH3 domains increase their diversity and regulate specific protein−protein interactions will be discussed.

MATERIALS AND METHODS

Sample Preparation. The recombinant wild-type and mutant PI3K SH3 domains were prepared as described previously (*16*, *18*). The concentration of proteins was determined by absorbance at 280 nm. The extinction coefficient of proteins denatured in 6 M guanidine hydrochloride (Gnd-HCl) solution was calculated according to the method of Gill and von Hippel (*19*). The values are 14 650 M^{-1} cm^{-1} for the wild type and 13 370 M^{-1} cm^{-1} for the Phe- or His-substituted mutants. The purified synthetic peptide, RLP1 (RKLPPRPSK−NH_2), was prepared as described previously (*16*).

† This work was supported by Grants-in-Aid for Scientific Research to T.K. (13308039) and M.N. (10670115) from the Ministry of Education, Science, Sports, and Culture of Japan and the Joint Studies Program (1999−2000) of the Institute for Molecular Science. T.T. is supported by JSPS and TARA.

* To whom correspondence should be addressed. Phone: 81 564 55 7340. Fax: 81 564 55 4639. E-mail: teizo@ims.ac.jp.

‡ School of Medicine, Kanazawa University Faculty of Medicine.

§ University of Tsukuba.

|| School of Health Sciences, Kanazawa University Faculty of Medicine.

⊥ Okazaki National Research Institutes.

[1] Abbreviations: CD, circular dichroism; Gnd-HCl, guanidine hydrochloride; K_d, dissociation constant; PI3K, phosphatidylinositol 3-kinase; SH3, Src homology 3; UVRR, UV resonance Raman.

10.1021/bi011339g CCC: $20.00
Published on Web 11/27/2001

CD Measurements. CD spectra were recorded on a Jasco J-725 spectropolarimeter at 25 °C. The instrument was calibrated with *d*-10-camphorsulfonic acid. CD spectra were acquired for a light path of 1 mm at a scan speed of 50 nm min^{-1} with a 1 nm slit width and a 1 s response time. For each experiment, 20 spectra were obtained and averaged. CD data were expressed in terms of mean residue molar ellipticity (θ) (deg cm^2 $dmol^{-1}$). Sodium sulfate was used for an internal intensity standard in UVRR spectroscopy and, therefore, was added to CD samples to compare directly UVRR and CD data. Sample concentration was 0.05 mM SH3 with or without 0.2 mM RLP1 (for the far-UV region: ca. 200−250 nm) or 0.2 mM SH3 with or without 0.8 mM RLP1 (for the near-UV region: ca. 250−300 nm) in 50 mM Tris-HCl (pH 7.2) containing 100 mM sodium sulfate. Under this condition, ca. 80−95% (for 0.05 mM SH3) or more than 95% (for 0.2 mM SH3) of PI3K SH3 and its mutants was estimated to be in the RLP1-bound form on the basis of their dissociation constant (K_d) values (*18*). Gnd-HCl was added to the final concentration of 6 M for the denatured condition.

UVRR Measurements. UVRR spectra were obtained with a XeCl excimer laser-pumped dye laser system (EMG103-MSC/LPX120 and FL2002/SCANMATE, Lambda Physik) (*14*, *20*). The 308-nm line from a XeCl excimer laser (operated at 100 Hz) was used to excite coumarin 480, and the 470-nm output from the dye laser was frequency-doubled with a β-BaB_2O_4 crystal to generate 235-nm pulses. The Raman excitation radiation (2−3 mJ cm^{-2}) was directed into the sample solution contained in a spinning cell from a lower front side. The scattered radiation was collected with Cassegrainian optics with f/1.1 and dispersed with an asymmetric double monochromator (Spex 1404) in which the gratings in the first and second dispersion steps are 2400 (holographic) and 1200 grooves mm^{-1} (machine-ruled, 500-nm blaze), respectively. The Raman scattering was detected by an intensified photodiode array (PC-IMD/C5222-0110G, Hamamatsu Photonics). The temperature of a sample solution was kept at room temperature by flushing with cooled nitrogen gas against the cell. One spectrum is a sum of 400 exposures, each exposure accumulating the data for 0.8 s. The spinning cell was moved vertically by 1 mm after acquiring each spectrum to shift a laser illumination spot on the sample. The sample was replaced with a fresh one after obtaining eight spectra. A UVRR spectrum presented is a sum of 24 spectra. Raman shifts were calibrated with cyclohexane. Sample concentration was 0.2 mM SH3 with or without 0.8 mM RLP1 in 50 mM Tris-HCl (pH 7.2) containing 100 mM sodium sulfate. Under this condition, more than 95% of the measured SH3 domains was estimated to be in the RLP1-bound form. The 982-cm^{-1} band of sulfate ions was used to normalize the ordinate scales of spectra and to calculate differences. In the 235-nm excited UVRR spectra, L-Tyr and L-Trp do not have any detectable RR bands in the region of ca. 900−950 cm^{-1} (data not shown). Therefore, the small spectral differences in this region were regarded as noise and used to evaluate the signal-to-noise ratios of the results.

RESULTS

CD Analysis. Figure 1 shows the UV CD spectra of PI3K SH3 in the native and denatured conditions. In the near-UV region, CD bands of proteins are generally dominated by

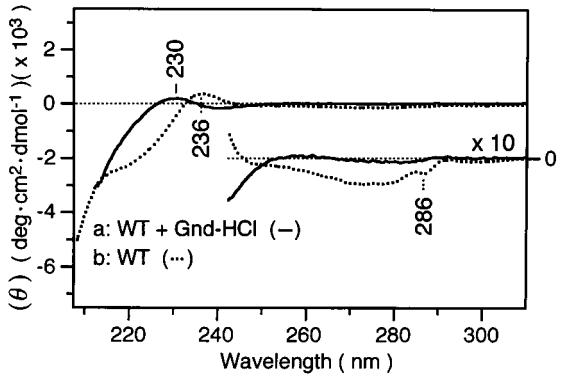

FIGURE 1: UV CD spectra of the native (dotted line) and denatured (solid line) PI3K SH3 domain in 50 mM Tris-HCl (pH 7.2) containing 100 mM sodium sulfate. For the denatured condition, Gnd-HCl was added to the final concentration of 6 M.

contributions from aromatic side chains and disulfides (*21*−*23*). Since PI3K SH3 contains seven Tyr (Tyr6, Tyr8, Tyr12, Tyr14, Tyr59, Tyr73, and Tyr76), one Trp (Trp55), two Phe (Phe42 and Phe69), and no Cys residues, the CD bands in the near-UV region are attributed to the asymmetrical surroundings of these aromatic side chains. The loss of near-UV CD bands in the denatured condition indicates that the asymmetric environments around aromatic residues in the native state are disrupted upon unfolding. In the far-UV region, a peak at 236 nm disappeared, and spectral features typical of an unordered polypeptide backbone were observed in the denatured condition, which are characterized by a weak positive or negative band near 220 nm contiguous to a strong negative band in the shorter wavelength (*22*). These observations indicate that the CD bands both in the near-UV and 230-nm regions are sensitive to environmental and structural changes of the SH3 domain, and thus it is useful to monitor them.

Figure 2 shows the UV CD spectra of the wild type and the Y → F mutants of PI3K SH3 with or without RLP1. Spectral changes induced by RLP1 are clearly seen in their difference spectra shown in Figure 3. The difference spectra of the Y12F, Y14F, and Y73F mutants (parts D, E, and G of Figure 3, respectively) were totally different from that of the wild type (Figure 3A) and from each other. The other Y → F mutants showed difference spectra quite similar to that of the wild type in both the near- and far-UV regions.

UVRR Analysis. The Y → F mutants of Tyr12, Tyr14, and Tyr73 were further subjected to the 235-nm excited UVRR analysis and compared with the wild type (Figure 4). The Y76F mutant, which had a similar CD spectral change to that of the wild type upon the RLP1 addition (Figure 3H), was also used for comparison. At this excitation wavelength, a strong enhancement is expected for the vibrational modes associated with Trp and Tyr residues, and the frequencies and intensities of these bands are known to be sensitive to side-chain structure, environmental hydrophobicity and polarity, and a hydrogen bonding state (*7*−*10*). The Raman bands of the wild type and the mutants were seen at 1207 (Y7a), 1173 (Y9a), 1010 (W16), 854 and 830 (Tyr doublet, Y1 and 2 × Y16a), and 759 cm^{-1} (W18). In the case of RLP1, which has no aromatic residues, only the 982-cm^{-1} band of the sulfate ions was observed (Figure 4P).

The addition of RLP1 brought about characteristic changes in each RR band. The spectral changes of the Y12F, Y73F,

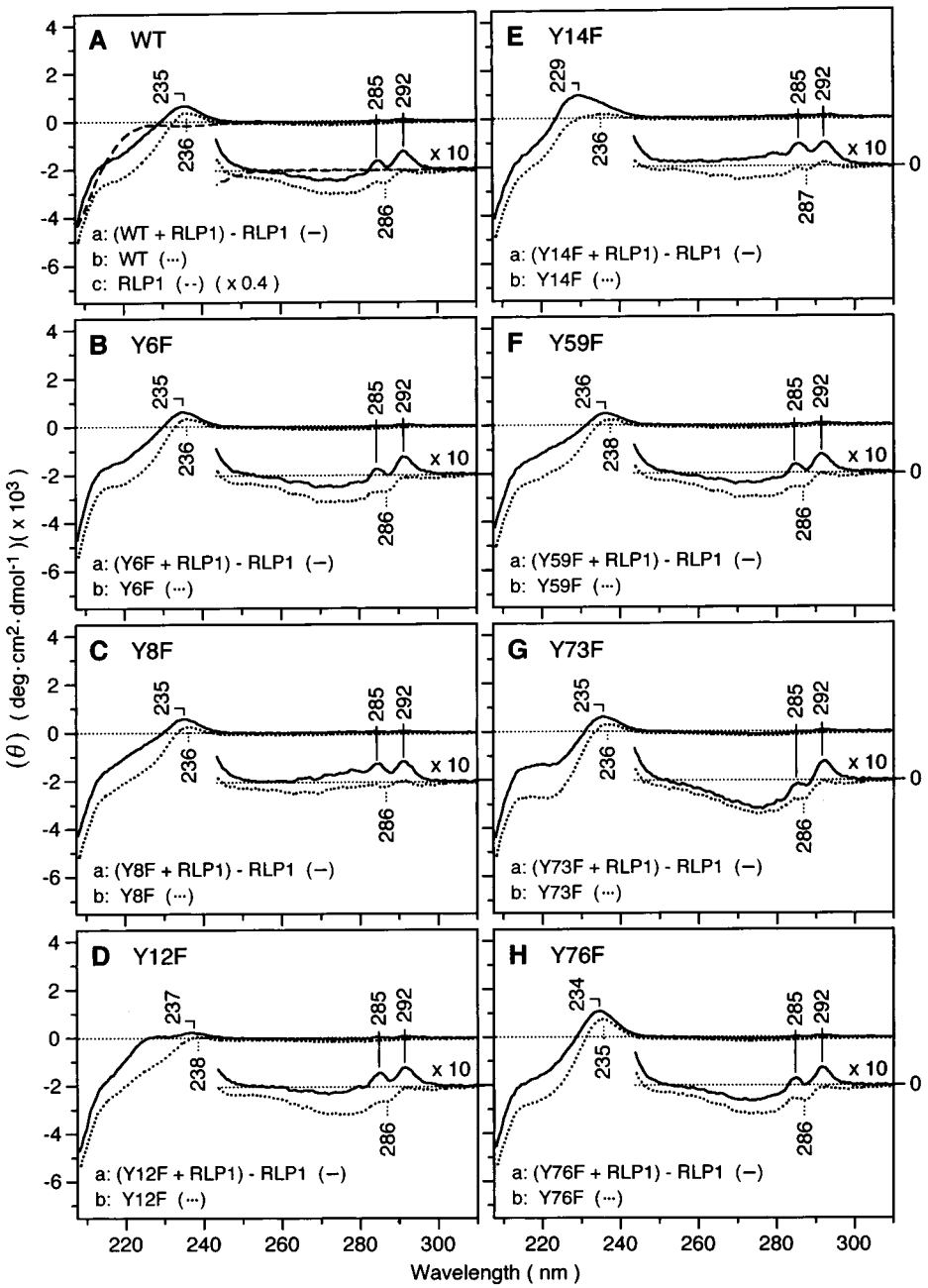

FIGURE 2: UV CD spectra of the PI3K SH3 domain and its Y → F mutants with (solid line) or without (dotted line) RLP1: (A) wild type; (B) Y6F mutant; (C) Y8F mutant; (D) Y12F mutant; (E) Y14F mutant; (F) Y59F mutant; (G) Y73F mutant; (H) Y76F mutant. The spectrum of free RLP1 is drawn with a dashed line in (A) and is subtracted from those of the mixture of the SH3 domain and RLP1. The spectral intensity of RLP1 should be drawn in 2.5 times larger when the ordinate scale is represented in terms of mean residue molar ellipticity, because it consists of nine residues (90 residues for the SH3 domain) and its concentration was 4 times higher than that of the SH3 domain. The sample concentration was 0.05 mM SH3 with or without 0.2 mM RLP1 (0.2 mM SH3 with or without 0.8 mM RLP1 for 10-fold expanded spectra) in 50 mM Tris-HCl buffer (pH 7.2) containing 100 mM sodium sulfate.

and Y76F mutants were similar to that of the wild type: intensity decrements of W16 (ca. 10−15%) and W18 (ca. 15−20%), intensity increments of Y7a (ca. 5−10%), Y9a (ca. 5−10%), and Tyr doublet (ca. 5−10%), and a frequency downshift by 2 cm^{-1} of W18. The spectral differences are much larger than the level of noise (see Materials and Methods) and thus thought to be significant.

The intensity increments of Trp (or Tyr) Raman bands indicate that a Trp (or Tyr) residue is placed in a more hydrophobic (less polar) environment and may have hydrogen bonding with a proton acceptor (*24*−*26*). On the other hand, the frequency of W18 is known to be upshifted when the indole NH site is more strongly hydrogen bonded with a proton acceptor in a hydrophobic environment (*25*). Therefore, in the Y12F, Y73F, and Y76F mutants as well as the wild type, Trp55, a unique Trp residue in PI3K SH3, is placed in a less hydrophobic (more polar) environment, and its hydrogen bonding is reduced or depleted, whereas a Tyr residue(s) is placed in a more hydrophobic (less polar) environment and may have hydrogen bonding.

On the contrary, in the Y14F mutant, intensity changes of the Trp Raman bands as well as the Tyr doublet band were not so obvious, although the W18 band showed the same frequency downshift (2 cm^{-1}) as the case of the wild

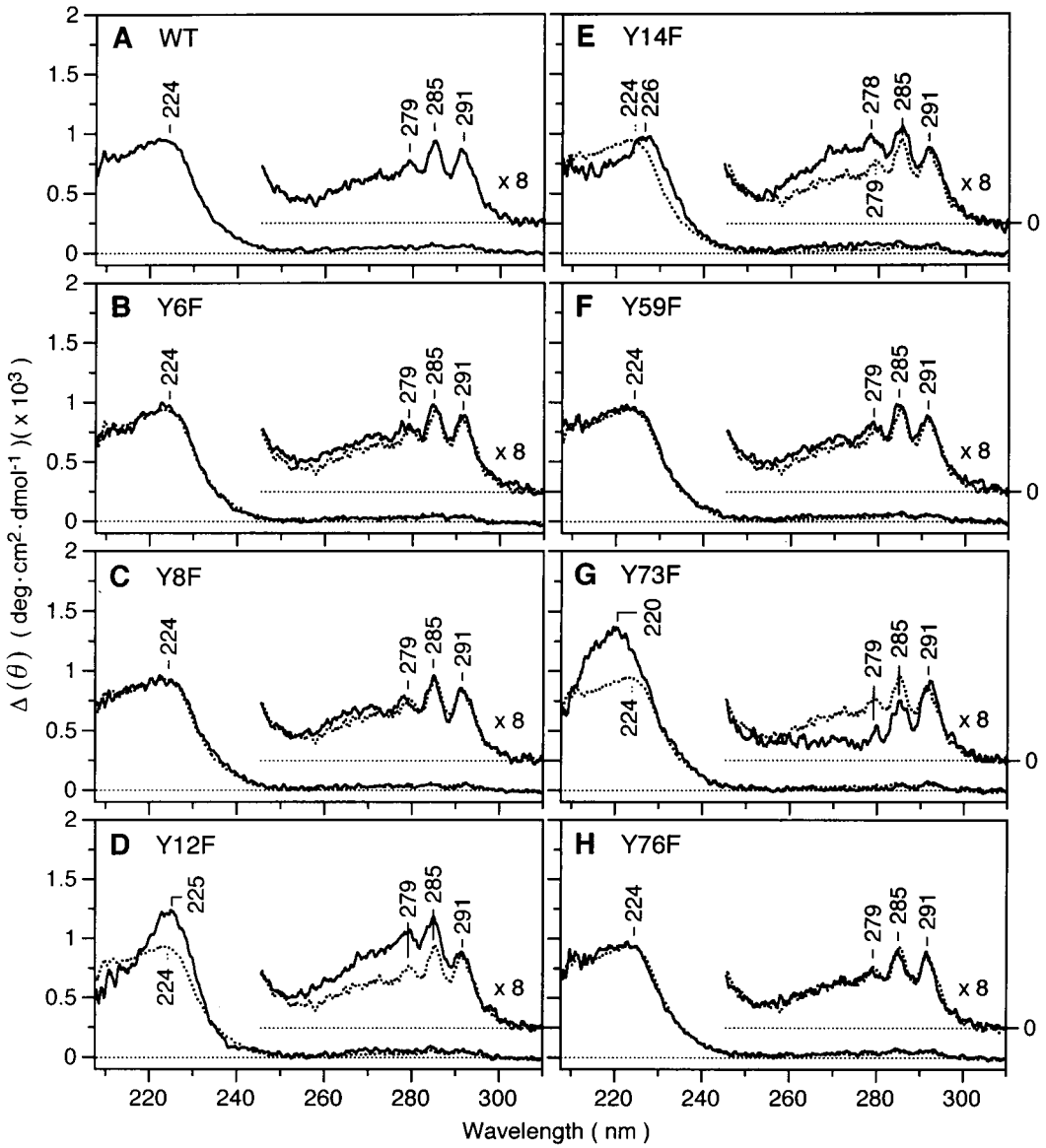

FIGURE 3: UV CD difference spectra of the PI3K SH3 domain and its Y → F mutants between with and without RLP1: (A) wild type; (B) Y6F mutant; (C) Y8F mutant; (D) Y12F mutant; (E) Y14F mutant; (F) Y59F mutant; (G) Y73F mutant; (H) Y76F mutant. In panels B−H, the difference spectra of the wild type between with and without RLP1 are drawn in a dotted line for comparison.

type (Figure 5). This indicates that, in the Y14F mutant, the RLP1-induced environmental change of Trp55 is not so prominent as in the wild type, although its hydrogen bonding is similarly reduced or depleted. Also, the RLP1-induced change of a Tyr residue(s) in the Y14F mutant is different from that in the wild type.

It is also noteworthy that there are small differences in the frequency of a difference peak derived from Y9a among the wild type and the Y12F, Y14F, Y73F, and Y76F mutants: 1168−1169 cm^{-1} for the wild type and the Y14F and Y76F mutants and 1164−1165 cm^{-1} for the Y12F and Y73F mutants. The Y9a frequency is known to be sensitive to the dihedral angle (τ_{CO}) formed between the COH and benzene planes (*27*); the larger τ_{CO} angle gives the lower frequency (1177−1179 cm^{-1} for 1.4°, 1174 cm^{-1} for 11.7°, and 1173 cm^{-1} for 17.4°). Therefore, the τ_{CO} angle of a Tyr residue in the Y12F or Y73F mutant is thought to be larger than that in the wild type when bound to RLP1.

The UVRR spectral changes in the Y6F, Y8F, and Y59F mutants induced by RLP1 were also examined. The difference spectra of these mutants between with and without RLP1 were similar to that of the wild type, as was observed in the Y76F mutant (see Supporting Information).

Y14H Mutant. To investigate effects of the mutation at Tyr14 in detail, we measured the CD and UVRR spectra of the Y14H mutant with or without RLP1. His was selected for the substitution because its side chain has a ring structure of a similar size with Tyr and Phe but has a more hydrophilic character than them.

The UV CD spectral change of the Y14H mutant upon the RLP1 binding is shown in Figure 6. The addition of RLP1 to the Y14H mutant induced a larger change in the near-UV region than the case of its addition to the wild type or the Y14F mutant (Figure 6B). Regarding that Phe and His residues generally do not contribute to the CD bands longer than 270 nm (*21*), the spectral differences between the Y14F and Y14H mutants are due to the fact that different environmental and structural changes are induced by RLP1 to Trp55 and/or other Tyr residues than Tyr14.

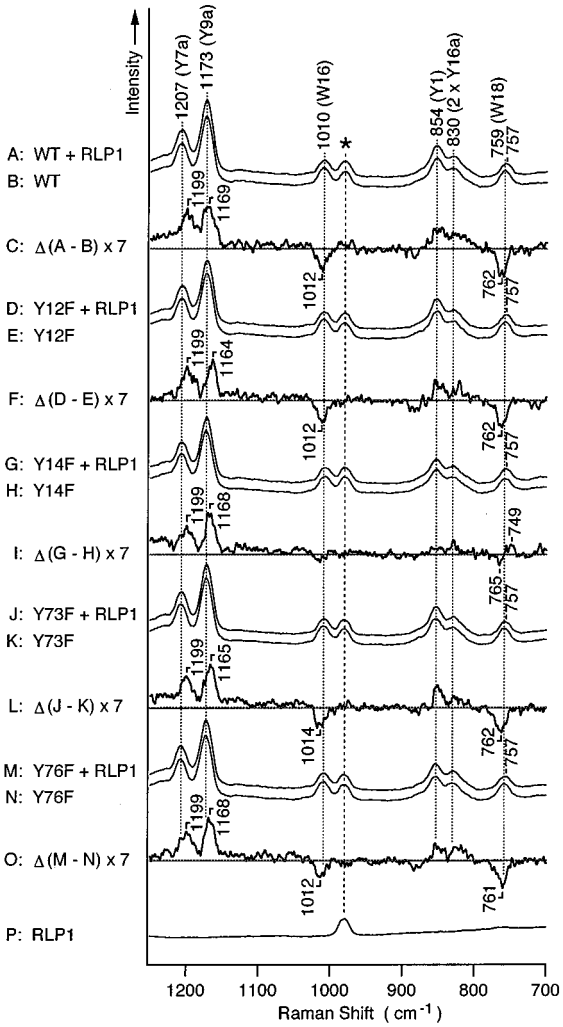

FIGURE 4: The 235-nm excited UVRR spectra of the wild type (A−C) and the mutants of Y12F (D−F), Y14F (G−I), Y73F (J−L), and Y76F (M−O) in the presence (A, D, G, J, and M) or absence (B, E, H, K, and N) of RLP1, and their 7-fold difference spectra (C, F, I, L, and O). The spectrum of RLP1 (P) is also shown. The Raman bands of Trp and Tyr vibrations are labeled by W and Y, respectively, at the top with their mode designations established by Harada and Takeuchi (*8*). The asterisk denotes the Raman band of sulfate ions (982 cm^{-1}) used as an internal intensity standard. The sample concentration was 0.2 mM SH3 with or without 0.8 mM RLP1 in 50 mM Tris-HCl buffer (pH 7.2) containing 100 mM sodium sulfate.

Figure 7 shows the UVRR spectra of the Y14H mutant with or without RLP1. There were no significant differences between the Y14H and Y14F mutants before the RLP1 addition (Figure 7F). However, spectral changes induced by RLP1 were quite different from each other (Figure 7C,E). Upon the RLP1 addition, the intensity of Trp Raman bands in the Y14H mutant decreased like those in the wild type (Figure 7C,D), but there were no discernible changes in Tyr Raman bands. The W18 band of the Y14H mutant showed the same frequency downshift (2 cm^{-1}) as the cases of the wild type and the Y14F mutant (Figure 5).

DISCUSSION

Assignment of Tyr Residues Involved in the Ligand Recognition. We recently constructed a series of Y → F mutants of PI3K SH3 and determined their binding affinities for RLP1 by CD analysis (Table 1) (*18*); the K_d values of

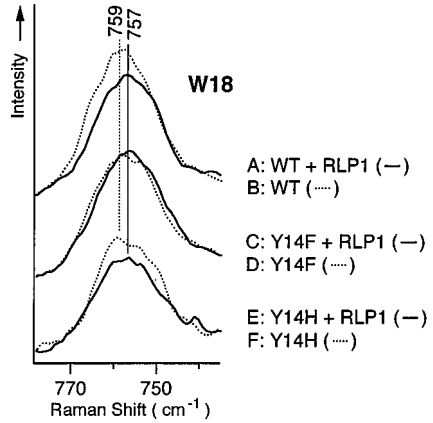

FIGURE 5: The expanded UVRR spectra of the W18 region of the wild type (upper), the Y14F mutant (middle), and the Y14H mutant (lower) in the presence (solid line) or absence (dotted line) of RLP1.

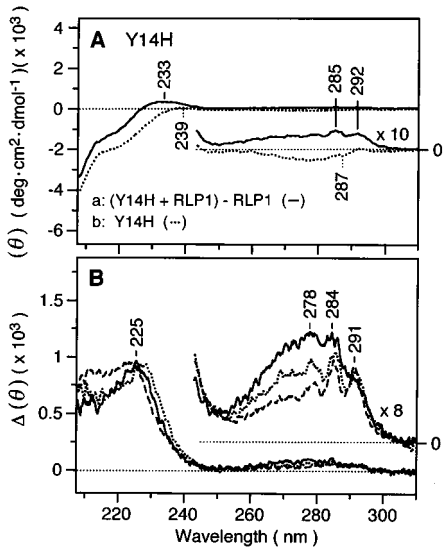

FIGURE 6: UV CD spectra of the Y14H mutant with (solid line) or without (dotted line) RLP1 (A), and their difference spectra (B). In panel B, the difference spectra between with and without RLP1 of the Y14H mutant (solid line) are drawn with those of the Y14F mutant (dotted line) and the wild type (dashed line). Experimental conditions were the same with those in Figures 2 and 3.

the Y12F, Y14F, and Y73F mutants are 17, 7, and 16 μM, respectively, and those of the wild type and the other Y → F mutants are 19−20 μM. These results indicate that the substitution of a Phe residue for a nonconserved Tyr residue (Tyr6, Tyr8, Tyr59, or Tyr76) does not cause any discernible change in the binding affinity, and that the alteration of a K_d value is small even in the substituent for a conserved Tyr residue (Tyr12, Tyr14, or Tyr73). Therefore, the Y → F mutations generally do not induce such large conformational changes as to deform the ligand binding cleft and disrupt the SH3−ligand interaction, and thus it is possible to assign a Tyr residue responsible for the ligand binding by comparing the CD and UVRR spectra of the wild type and the Y → F mutants with or without RLP1.

As shown in Figure 3, the RLP1 binding induced similar spectral changes among the Y → F mutants of the nonconserved Tyr residues (Tyr6, Tyr8, Tyr59, and Tyr76) (parts B, C, F, and H, respectively). In addition, their spectral changes were almost identical to that of the wild type (Figure 3A). On the contrary, distinct spectral changes were observed

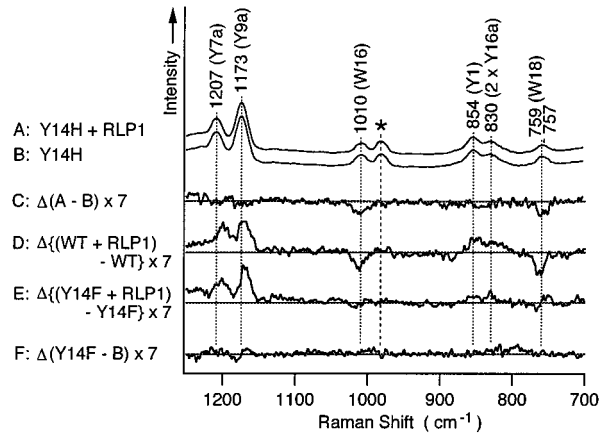

FIGURE 7: The 235-nm excited UVRR spectra of the Y14H mutant in the presence (A) or absence (B) of RLP1, and their 7-fold difference spectra (C). The 7-fold difference spectra of the wild type and the Y14F mutant between with and without RLP1 (D and E, respectively) and that between Y14F and Y14H mutants (F) are also shown. Experimental conditions were the same with those in Figure 4.

Table 1: Dissociation Constants of PI3K SH3 and Its Mutants for RLP1[a]

PI3K SH3	K_d (μM)	PI3K SH3	K_d (μM)
wild type	19	Y59F	20
Y6F	20	Y73F	16
Y8F	20	Y76F	19
Y12F	17	Y14H	33
Y14F	7		

[a] Reported previously by Okishio et al. (*18*). K_d values were obtained by CD measurements.

in the mutants of the conserved Tyr residues (Tyr12, Tyr14, and Tyr73) (parts D, E, and G of Figure 3, respectively). Therefore, we concluded that all of the conserved Tyr residues participate in the ligand recognition. Yu et al. (*17*) determined the solution structure of PI3K SH3 complexed with RLP1 and reported that the binding energy for complex formation is mostly derived from the following hydrophobic contacts: Leu3 of RLP1 with Trp55, Pro70, Thr72, and Tyr73; Pro4 of RLP1 with Tyr14, Trp55, Pro70, and Tyr73; Pro7 of RLP1 with Tyr12. Their results show that the three Tyr residues (Tyr12, Tyr14, and Tyr73) as well as Trp55 are involved in the RLP1 binding, which is consistent with our CD analysis.

The Y → F mutants were further subjected to UVRR analysis and compared with the wild type. The RLP1 binding induced similar spectral changes among the Y → F mutants of the nonconserved Tyr residues (Tyr6, Tyr8, Tyr59, and Tyr76) (Supporting Information and Figure 4O) and the wild type (Figure 4C), as was observed in the CD analysis. This suggests that the nonconserved Tyr residues are not much involved in the RLP1 binding. For the Y12F and Y73F mutants, their UVRR spectral changes induced by RLP1 were almost identical to that of the wild type (parts C, F, and L of Figure 4). This indicates that the Y12F and Y73F mutants interact with RLP1 in a rather similar way to the wild type and that the contribution of Tyr12 and Tyr73 to the spectral changes of Tyr Raman bands in the wild type are small.

On the contrary, the UVRR spectral change of the Y14F mutant was significantly different from that of the wild type (Figure 4C,I). It suggests that Tyr14 contributes most to the RLP1 recognition by the wild type. However, the contribution of Tyr14 could not be evaluated exactly because the Y14F mutant interacts with RLP1 in a different way from the wild type, as is indicated by the different appearance of Trp Raman bands (W16 and W18) between them. Therefore, we used the Y14H mutant to assess the contribution of Tyr14. This mutant has a K_d value of 33 μM for RLP1 (Table 1) (*18*) and thus, like the Y → F mutants, maintains a functional ligand binding surface. In addition, the Y14H mutant gives similar spectral changes in Trp Raman bands to the wild type, which indicates the resemblance of their RLP1 binding modes. In this binding state, spectral changes in Tyr Raman bands of the Y14H mutant were not detected due to the absence of Tyr14. Accordingly, we concluded that Tyr14 is most critical for the RLP1-induced spectral changes of Tyr Raman bands in the wild-type SH3 domain.

Table 2: Dissociation Constants of RLP1 and Its Mutants for PI3K SH3[a]

RLP1	K_d (μM)	RLP1	K_d (μM)
wild type	9.1	P4A	140
R1A	98.0	P5A	16.5
K2A	9.7	R6A	29
L3A	37	P7A	53

[a] Reported previously by Yu et al. (*17*). K_d values were determined by fluorescence measurements.

A possible factor responsible for the spectral changes in Tyr Raman bands is a hydrophobic contact between Tyr14 and Pro4 of RLP1. The effect of Y → F mutation on the binding affinity for RLP1 is most prominent in the Y14F mutant (K_d, 7 μM), and the affinity is decreased in the Y14H mutant (K_d, 33 μM) where more hydrophilic substitution is introduced (Table 1) (*18*). On the other hand, the K_d values of the Y12F and Y73F mutants (17 and 16 μM, respectively) are similar to that of the wild type (19 μM) (Table 1) (*18*). These results provide evidence that Tyr14 is the most crucial Tyr residue for the proper hydrophobic interaction with RLP1. This is reinforced by the results obtained by Yu et al. (*17*), who found that the binding affinities for the SH3 domain are decreased by ca. 4-, 15-, and 6-fold in the RLP1 mutants of L3A (Leu3 → Ala), P4A (Pro4 → Ala), and P7A (Pro7 → Ala), respectively (Table 2).

Alteration of the hydrogen bonding state of Tyr14 may also contribute to the RLP1-induced intensity changes in Tyr Raman bands. In the ligand-free structure, H_η and O_η of Tyr14 are close to $O_{\delta 2}$ of Asp21 and the backbone amide proton of Glu17 or Arg18, respectively (*28*). In the RLP1-bound structure, they are in the proximity of the backbone carbonyl oxygen of Lys15 and $H_{\eta 1}$s or H_ϵ of Arg1 of RLP1, respectively (*17*). Therefore, the hydrogen bonding state of Tyr14 appears to be different between the uncomplex and complex states.

Modulation of the Ligand Binding Mode. The RLP1 addition caused distinct environmental and structural changes of Trp55 and a Tyr residue(s) among the wild type, the Y14F mutant, and the Y14H mutant. As for the wild type, the intensity of Trp Raman bands was decreased, and the frequency of W18 was downshifted (Figure 5A,B). This is likely because Trp55 becomes surrounded by proton donors of RLP1 such as a guanidino side chain of Arg1 and backbone amino or amide groups of Arg1, Lys2, and Leu3 (*16*, *17*). This is also the case with the Y14H mutant, which

shows similar changes of Trp Raman bands upon RLP1 binding (Figure 5E,F). In the Y14F mutant, the intensity change of Trp Raman bands was not observed, although the frequency of W18 was downshifted (Figure 5C,D). This suggests that the enclosure of Trp55 by the proton donors of RLP1 may be weak in the Y14F mutant.

The intensity of Tyr Raman bands in the wild type was increased by the RLP1 addition (Figure 7D). This is due to the environmental and structural changes of Tyr14 caused by RLP1. The loss of intensity changes of Tyr Raman bands in the Y14H mutant (Figure 7C) provides evidence that no other Tyr residues than Tyr14 are much involved in the RLP1 recognition by the wild type. In contrast with the wild type, the intensity increments of Tyr Raman bands in the Y14F mutant (Figure 7E) denote that some Tyr residue(s) other than Tyr14 is placed in a more hydrophobic (less polar) environment and may have hydrogen bonding. The responsible Tyr residue in the Y14F mutant is likely to be Tyr12 and/or Tyr73, because Tyr residues which participate in the ligand recognition are limited to Tyr12, Tyr14, and Tyr73.

As discussed above, the wild type and the Y14H mutant are similar to each other but different from the Y14F mutant in the RLP1 binding mode. The factors capable of affecting the SH3−RLP1 interaction are a hydrophobic contact between Tyr14 and Pro4 of RLP1 as well as a hydrogen bond between a phenolic OH group of Tyr14 and a guanidino group of Arg1 of RLP1. Models showing possible effects of the Y14F and Y14H mutations are depicted in Figure 8. In the wild type, the SH3−RLP1 interaction appears to be stabilized in part by a hydrophobic contact between Tyr14 and Pro4 of RLP1 as well as a hydrogen bond between O_η of Tyr14 and $H_{\eta 11}$ (or $H_{\eta 12}$) of Arg1 of RLP1. Trp55 is surrounded by proton donors such as a guanidino side chain of Arg1 and backbone amino or amide groups of Arg1, Lys2, and Leu3 (Figure 8A). The Y14F mutation probably strengthens the hydrophobic interaction with Pro4. In addition to this effect, depletion of the hydrogen bonding with Arg1 may affect the RLP1 binding mode, in which Trp55 is less surrounded by proton donors (Figure 8B). In the Y14H mutant, the hydrophobic interaction with Pro4 may be weak. However, preservation of the hydrogen bond between His14 and Arg1 may minimize the effect of the mutation on the RLP1 binding mode (Figure 8C).

The SH3−RLP1 interaction may be somewhat affected by the Y → F mutation at Tyr12 or Tyr73, because the Y9a difference peaks of the Y12F and Y73F mutants were downshifted by 4−5 cm^{-1} as compared with that of the wild type or the other mutants (Figure 4 and Supporting Information). The most plausible Tyr residue responsible for the spectral changes of Tyr Raman bands in the Y12F and Y73F mutants is Tyr14, because UVRR analyses suggest that the Y12F and Y73F mutants interact with RLP1 in a rather similar way to the wild type and that the contribution of Tyr12 and Tyr73 to the spectral changes in Tyr Raman bands are small. Accordingly, the τ_{CO} angle of Tyr14 in these mutants is likely to be larger than that in the wild type when bound to RLP1.

Mechanisms by Which SH3 Domains Produce Diversity and Specificity. Alteration of the general ligand binding mode by the amino acid substitutions for the conserved Tyr residues in PI3K SH3 gives an insight into how each SH3 domain can produce diversity and specificity at the same time. It is well known that specific signaling is achieved by the high affinity and specific binding of a particular SH3 domain to its ligand. Several studies identified the ligand sequences which can bind to SH3 domains with high affinity and specificity (*29*−*31*). These ligands bind to SH3 domains in two opposite orientations (plus and minus) and typically have a consensus sequence of RXΦPXXP (class I) or PXΦPXR (class II) (Φ and X stand for hydrophobic and any amino acid residues, respectively) (*32*, *33*). The binding orientation is determined by the interaction between a conserved acidic residue in SH3 domains (Asp21 in PI3K SH3) and a basic residue in ligands (Arg1 in RLP1). It is likely that RLP1 binds to the Y14F and Y14H mutants in the same direction, because both Asp21 in the domain and Arg1 in RLP1 are preserved in these mutants. However, the present observation stresses that their ways to associate with RLP1 are different from each other, suggesting that the SH3−ligand interaction is so finely regulated and modulated by small structural changes in the hydrophobic cleft of the domain. This could be an additional mechanism to give variety to the ligand recognition by SH3 domains.

Prominent effect of a single mutation in a ligand binding site on both ligand specificity and a binding mode were clearly demonstrated in the Src SH2 domain. The wild-type Src SH2 domain binds the phosphopeptides containing

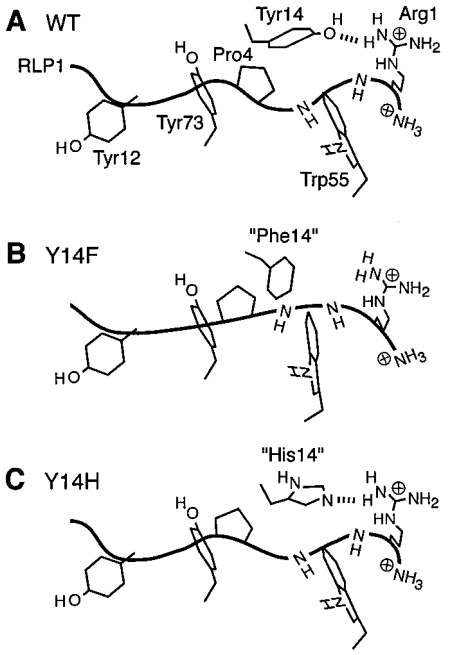

FIGURE 8: Models showing possible effects of the Y14F and Y14H mutations of PI3K SH3 on the SH3−RLP1 interaction. The side chains of Tyr12, Tyr14, Trp55, and Tyr73 of PI3K SH3 and those of Arg1 and Pro4 of RLP1 are depicted with the C_α backbone trace of RLP1. (A) In the wild type, the interaction is stabilized in part by a hydrophobic contact between Tyr14 and Pro4 of RLP1 as well as a hydrogen bond between O_η of Tyr14 and $H_{\eta 11}$ (or $H_{\eta 12}$) of Arg1 of RLP1. Trp55 is surrounded by proton donors of RLP1 such as a guanidino side chain of Arg1 and backbone amino or amide groups of Arg1, Lys2, and Leu3. (B) The Y14F mutation is likely to strengthen the hydrophobic interaction with Pro4. However, the mutation may cause the depletion of the hydrogen bonding with Arg1 and alter the RLP1 binding mode. (C) The hydrophobic contact between His14 and Pro4 in the Y14H mutant may be not so strong. However, preservation of the hydrogen bond between His14 and Arg1 may minimize the effect of the mutation on the RLP1 binding.

pYEEI (Glu at the +1 position, Glu at +2, and Ile at +3) motif in an extended conformation. However, a single substitution of Thr215 to Trp switches the sequence preference to an Asn requirement at the +2 position (*34*), and this mutated domain binds pYVNV-containing phosphopeptides in a β-turn conformation (*35*). Such alterations are also possible in SH3 domains. Our study suggests that ligand binding pockets of SH3 domains are so flexible and variable as to accommodate their structures to various ligands, and the fine-tuning and modulation of SH3−ligand interactions may play important roles in transducing signaling within cells.

ACKNOWLEDGMENT

We thank Drs. Stuart L. Schreiber and Hongtao Yu for providing the PI3K SH3-RLP1 coordinates prior to PDB release.

SUPPORTING INFORMATION AVAILABLE

The 235-nm excited UVRR spectra of the wild type (A−C), the mutants of Y6F (D−F), Y8F (G−I), and Y59F (J−L) in the presence (A, D, G, and J) or absence (B, E, H, and K) of RLP1, and their 7-fold difference spectra (C, F, I, and L). Experimental conditions were the same with those in Figure 4. This material is available free of charge via the Internet at http://pubs.acs.org.

REFERENCES

1. Kapeller, R., and Cantley, L. C. (1994) *BioEssays 16*, 565−576.
2. Vanhaesebroeck, B., and Waterfield, M. D. (1999) *Exp. Cell Res. 253*, 239−254.
3. Gout, I., Dhand, R., Hiles, I. D., Fry, M. J., Panayotou, G., Das, P., Truong, O., Totty, N. F., Hsuan, J., Booker, G. W., Campbell, I. D., and Waterfield, M. D. (1993) *Cell 75*, 25−36.
4. Barfod, E. T., Zheng, Y., Kuang, W.-J., Hart, M. J., Evans, T., Cerione, R. A., and Ashkenazi, A. (1993) *J. Biol. Chem. 268*, 26059−26062.
5. Harrison-Findik, D., Šuša, M., and Varticovski, L. (1995) *Oncogene 10*, 1385−1391.
6. Guinebault, C., Payrastre, B., Racaud-Sultan, C., Mazarguil, H., Breton, M., Mauco, G., Plantavid, M., and Chap, H. (1995) *J. Cell Biol. 129*, 831−842.
7. Tu, A. T. (1986) in *Spectroscopy of Biological Systems* (Clark, R. J. H., and Hester, R. E., Eds.) pp 47−112, John Wiley & Sons, Ltd., New York.
8. Harada, I., and Takeuchi, H. (1986) in *Spectroscopy of Biological Systems* (Clark, R. J. H., and Hester, R. E., Eds.) pp 113−175, John Wiley & Sons, Ltd., New York.
9. Kitagawa, T. (1992) *Prog. Biophys. Mol. Biol. 58*, 1−18.
10. Austin, J. C., Rodgers, K. R., and Spiro, T. G. (1993) *Methods Enzymol. 226*, 374−396.
11. Kaminaka, S., Ogura, T., and Kitagawa, T. (1990) *J. Am. Chem. Soc. 112*, 23−27.
12. Rodgers, K. R., Su, C., Subramaniam, S., and Spiro, T. G. (1992) *J. Am. Chem. Soc. 114*, 3697−3709.
13. Nagai, M., Wajcman, H., Lahary, A., Nakatsukasa, T., Nagatomo, S., and Kitagawa, T. (1999) *Biochemistry 38*, 1243−1251.
14. Nagatomo, S., Nagai, M., Tsuneshige, A., Yonetani, T., and Kitagawa, T. (1999) *Biochemistry 38*, 9659−9666.
15. Okishio, N., Fukuda, R., Nagai, M., Nagai, Y., Nagatomo, S., and Kitagawa, T. (1998) *J. Raman Spectrosc. 29*, 31−39.
16. Okishio, N., Nagai, M., Fukuda, R., Nagatomo, S., and Kitagawa, T. (2000) *Biopolymers 57*, 208−217.
17. Yu, H., Chen, J. K., Feng, S., Dalgarno, D. C., Brauer, A. W., and Schreiber, S. L. (1994) *Cell 76*, 933−945.
18. Okishio, N., Tanaka, T., Fukuda, R., and Nagai, M. (2001) *Biochemistry 40*, 119−129.
19. Gill, S. C., and von Hippel, P. H. (1989) *Anal. Biochem. 182*, 319−326.
20. Kaminaka, S., and Kitagawa, T. (1992) *Appl. Spectrosc. 46*, 1804−1808.
21. Strickland, E. H. (1974) *CRC Crit. Rev. Biochem. 2*, 113−175.
22. Woody, R. W. (1995) *Methods Enzymol. 246*, 34−71.
23. Kelly, S. M., and Price, N. C. (1997) *Biochim. Biophys. Acta 1338*, 161−185.
24. Hashimoto, S., Yabusaki, T., Takeuchi, H., and Harada, I. (1995) *Biospectroscopy 1*, 375−385.
25. Matsuno, M., and Takeuchi, H. (1998) *Bull. Chem. Soc. Jpn. 71*, 851−857.
26. Chi, Z., and Asher, S. A. (1998) *J. Phys. Chem. B 102*, 9595−9602.
27. Takeuchi, H., Watanabe, N., Satoh, Y., and Harada, I. (1989) *J. Raman Spectrosc. 20*, 233−237.
28. Koyama, S., Yu, H., Dalgarno, D. C., Shin, T. B., Zydowsky, L. D., and Schreiber, S. L. (1993) *Cell 72*, 945−952.
29. Rickles, R. J., Botfield, M. C., Zhou, X.-M., Henry, P. A., Brugge, J. S., and Zoller, M. J. (1995) *Proc. Natl. Acad. Sci. U.S.A. 92*, 10909−10913.
30. Lee, C.-H., Leung, B., Lemmon, M. A., Zheng, J., Cowburn, D., Kuriyan, J., and Saksela, K. (1995) *EMBO J. 14*, 5006−5015.
31. Pisabarro, M. T., and Serrano, L. (1996) *Biochemistry 35*, 10634−10640.
32. Feng, S., Chen, J. K., Yu, H., Simon, J. A., and Schreiber, S. L. (1994) *Science 266*, 1241−1247.
33. Lim, W. A., Richards, F. M., and Fox, R. O. (1994) *Nature 372*, 375−379.
34. Marengere, L. E. M., Songyang, Z., Gish, G. D., Schaller, M. D., Parsons, J. T., Stern, M. J., Cantley, L. C., and Pawson, T. (1994) *Nature 369*, 502−505.
35. Kimber, M. S., Nachman, J., Cunningham, A. M., Gish, G. D., Pawson, T., and Pai, E. F. (2000) *Mol. Cell 5*, 1043−1049.

BI011339G